# Leaping towards a saltatorial lifestyle? An unusually long-legged new species of *Rhombophryne* (Anura, Microhylidae) from the Sorata massif in northern Madagascar

Mark D. Scherz[1], Andolalao Rakotoarison[2], Oliver Hawlitschek[1,3], Miguel Vences[2], Frank Glaw[1]

1 *Zoologische Staatssammlung München (ZSM-SNSB), Münchhausenstr. 21, 81247 München, Germany*

2 *Zoologisches Institut, Technische Universität Braunschweig, Mendelssohnstraße 4, 38106 Braunschweig, Germany*

3 *Current address: IBE, Institut de Biologia Evolutiva (CSIC-Universitat Pompeu Fabra), Passeig Marítim de la Barceloneta 37, 08003 Barcelona, Spain*

http://zoobank.org/79F1E7CE-3ED3-4A6C-AA15-DC59AB3046B8

Corresponding author: *Mark D. Scherz* (mark.scherz@gmail.com)

## Abstract

## Key Words

The Madagascar-endemic microhylid genus *Rhombophryne* consists of a range of partly or completely fossorial frog species. They lead a poorly known, secretive lifestyle, and may be more diverse than previously thought. We describe a new species from the high altitude forests of the Sorata massif in north Madagascar with unusual characteristics for this genus; *R. longicrus* **sp. n.** has long, slender legs, unlike most of its fossorial or semi-fossorial congeners. The new species is closely related to *R. minuta*, a much smaller frog from the Marojejy massif to the southeast of Sorata with similarly long legs. We discuss the morphology of these species relative to the rest of the genus, and argue that it suggests adaptation away from burrowing and toward a more saltatorial locomotion and an accordingly more terrestrial lifestyle. If this is the case, then these frogs represent yet more ecological diversity within the already diverse Cophylinae. We recommend an IUCN Red List status of Endangered B1ab(iii) for *R. longicrus* **sp. n.**, because it is known only from a single site in a forested area of roughly 250 km², which is not yet incorporated into any protected area.

## Introduction

The microhylid frog genus *Rhombophryne* (Anura, Microhylidae, Cophylinae) is receiving renewed taxonomic attention in the wake of recent genetic barcoding efforts on the frogs of Madagascar. These DNA barcode studies revealed that less than 60% of the island's amphibian diversity might so far have been formally described (Vieites et al. 2009, Perl et al. 2014). The taxonomic gap between what has been described and the total diversity that exists is extreme in the cophyline microhylids, a Madagascar-endemic radiation of narrow-mouthed frogs. The cophyline genus *Rhombophryne* typifies the taxonomic gap: In 2007, it contained eight described species (Glaw and Vences 2007). Thirteen candidate species were identified by integrative inventories taking into account morphology and mtDNA and nuclear gene sequences (Wollenberg et al. 2008, Vieites et al. 2009, Perl et al. 2014). Still more have been discovered by additional fieldwork. Five of these have been described recently (D'Cruze et al. 2010, Glaw et al. 2010, Scherz et al. 2014, 2015), facilitated and accelerated by integrative approaches. These approaches are the key to closing the taxonomic gap in Madagascar's amphibians, which is in turn key to understanding and protecting them.

Repeated swapping of ecological niches (i.e. transitions between gross ways of life, such as between terrestrial and arboreal lifestyles) has led to high ecological diversity in the Cophylinae (Andreone et al. 2005, Wollenberg et al. 2008). The genus *Rhombophryne* is genetically most closely related to the dwarf frogs of the genus *Stumpffia* but

is morphologically very similar to *Plethodontohyla* (Andreone et al. 2005). *Rhombophryne* contains obligate and facultative burrowing frogs (Andreone et al. 2005, Wollenberg et al. 2008), and the enigmatic *R. minuta*, the ecology of which we discuss below. *Stumpffia*, a genus in need of revision, consists of mostly terrestrial dwarf frogs, some of which number among the smallest frogs in the world (Glaw and Vences 2007). Recently, Peloso et al. (2015) proposed the synonymy of *Stumpffia* and *Rhombophryne*. However, we here refrain from adopting their changes pending further investigation, as these genera are morphologically distinct. *Plethodontohyla* species resemble *Rhombophryne* more closely in size, but consist of a mixture of probably facultative burrowers and arboreal or semi-arboreal climbers. Reasons for this ecological flexibility, and the ancestral states of the genera, have so far been poorly explored (Andreone et al. 2005).

Here, we describe a new *Rhombophryne* clearly distinct from all other known species, although phylogenetically nested. We describe its skeleton by means of micro-computed tomography (micro-CT), revealing additional differences to the other *Rhombophryne* species for which skeletal data are available (Scherz et al. 2014, 2015, unpublished results). We discuss the implications of this potentially novel morphology for the evolution of the genus *Rhombophryne*, and highlight the need for herpetological survey work in less accessible areas of Madagascar.

## Materials and methods

Specimens were collected, euthanized, fixed in 90% ethanol and transferred to 70% ethanol for long-term storage. One specimen was deposited in the Université d'Antananarivo Département de Biologie Animale (UADBA), and the other in the Zoologische Staatssammlung München (ZSM).

In this work we refer to the species *R. ornata* and *R. tany*. Their descriptions are in press (Scherz et al. 2015), and we therefore give the disclaimer that the use of these two names here should be considered conditional, and these two names herein are not made nomenclaturally available, in accordance with Articles 8.3 and 15.1 of the International Code of Zoological Nomenclature (ICZN 1999).

Morphological measurements were taken with a digital calliper to 0.01 mm and rounded to the nearest 0.1 mm for presentation here. Fig. 1 shows our measurement scheme except cumulative measures (HIL, FORL, and FOTL). Abbreviations are used as follows: SVL (snout–vent length), HW (maximum head width), HL (head length, from the maxillary commissure to the anterior-most point of the mouth), ED (horizontal eye diameter), END (eye–nostril distance), NSD (nostril–snout tip distance), NND (internarial distance), TDH (horizontal tympanum diameter), TDV (vertical tympanum diameter), HAL (hand length, from the metacarpal–radioulnar articulation to the tip of the longest finger), LAL (lower arm length, from the carpal–radioulnar articulation to the centre of the radioulna–humeral articulation), UAL (upper arm length, from the centre
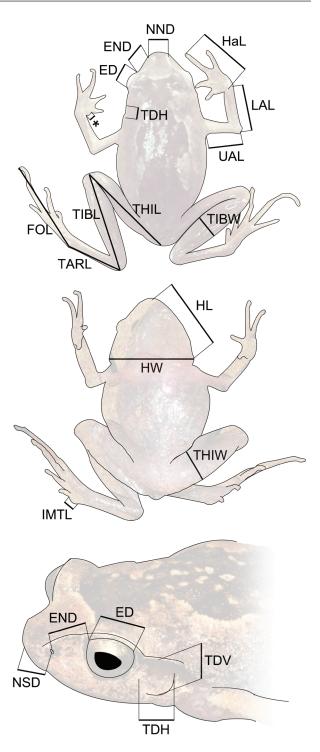


**Figure 1.** Measurement scheme used to measure *Rhombophryne longicrus* sp. n. and congeners for this study. Abbreviations are explained in Materials and Methods, as are cumulative measures such as forelimb and hindlimb length. * indicates IMCL.

of the radioulna–humeral articulation to the trunk, measured along the posterior aspect of the arm), FORL (forelimb length, given by the sum of HAL, LAL, and UAL), FOL (foot length, from the tarsal–metatarsal articulation to the tip of the longest toe), TARL (tarsal length, from the tarsal–metatarsal articulation to the tarsal–tibiofibular articulation), FOTL (foot length including tarsus, from the

tibiotarsal articulation to the tip of the longest toe, given by the sum of FOL and TARL), TIBL (tibiofibula length), TIBW (tibiofibula width at thickest point, measured in dorsal aspect), THIL (thigh length, from the vent to the femoral–tibiofibular articulation), THIW (thigh width at thickest point, measured in supine position), HIL (hindlimb length, given by the sum FOL, TARL, TIBL, and THIL), IMCL (maximum length of inner metacarpal tubercle), IMTL (maximum length of the inner metatarsal tubercle).

Micro-CT scanning was carried out on a nanotom m (GE Measurement & Control, Wunstorf, Germany). The holotype of the new species, ZSM 1630/2012, was mounted on a polystyrene board inside a sealed polyethylene vessel, and secured in place using small wooden struts and additional polystyrene. A small volume of 80% ethanol was added to achieve air saturation, preventing desiccation of the specimen. The vessel was mounted on a polyvinylchloride tube, and placed inside the micro-CT scanner. Scanning was conducted at a voltage of 140 kV and a current of 80 mA, with a timing of 500 ms for 20 minutes (2440 projections). Scan data were assembled in phoenix DATOS|X 2 RECONSTRUCTION CT software (GE Measurement & Control, Wunstorf, Germany) and visualised in VG STUDIO MAX 2.2 (Volume Graphics GmbH, Heidelberg, Germany) and subsequently processed into a 3D surface render in AMIRA 5.4.5 (FEI Visualization Sciences Group, Burlington MA, USA). Skeletal description is based on both surface and volume renderings of micro-CT data, due to artefacts produced in surface rendering. Readers are advised that micro-CT scanning does not render poorly calcified structures, especially cartilage. Cartilages are therefore omitted from the osteological description below and the respective figures; additional specimens will need to be cleared and stained in order to assess cartilaginous characters of these frogs. We provide a PDF-embedded interactive 3D model of the skeleton of the holotype as Suppl. material 1. Osteological terminology follows Trueb (1968, 1993). Skull ratio measurements were calculated from high resolution TIFF images of prepared models in ImageJ 1.48v (Schneider et al. 2012).

We extracted total genomic DNA from ethanol-preserved tissue samples using proteinase K digestion (final concentration 1 mg/mL) and a standard salt extraction protocol (Bruford et al. 1992). We amplified a fragment of the mitochondrial large ribosomal subunit or 16S rRNA (16S) via polymerase chain reaction (PCR) using the primers 16Sar-L and 16Sbr-H (Palumbi et al. 1991). Sequences were resolved on an ABI 3130xl automated DNA sequencer (Applied Biosystems) and newly determined sequences were deposited in GenBank (accession numbers KR025897 and KR025898).

We calculated a phylogenetic tree from the 16S sequences by Bayesian inference (BI) with MRBAYES 3.2 (Ronquist et al. 2012) after determining a GTR+I+G substitution model as best fitting the data using JMODELTEST (Darriba et al. 2012). We considered all sections of the 16S gene with more than two consecutive gaps in one or more sequences as ambiguous and excluded these sections from the alignment (total alignment length after exclusion: 397 nucleotides). Explorative analyses including these stretches resulted in an identical topology and similar support values for all nodes supported with PP > 0.9. We ran two independent analyses for 20 million generations, each comprising four Markov Chains (three heated and one cold), and sampled every 10,000 generations. Chain mixing and stationarity was assessed by examining the standard deviation of split frequencies and plotting the –lnL per generation using TRACER 1.6 software (Rambaut et al. 2014). Results were combined to obtain a 50%-majority rule consensus tree and the respective posterior probabilities of nodes, after discarding 25% of the generations as burn-in (all compatible nodes with probabilities <0.5 kept).

## Results

The new species described below is phylogenetically nested in the genus *Rhombophryne* (Fig. 2) and placed as sister to *R. minuta* with strong support. The relatively
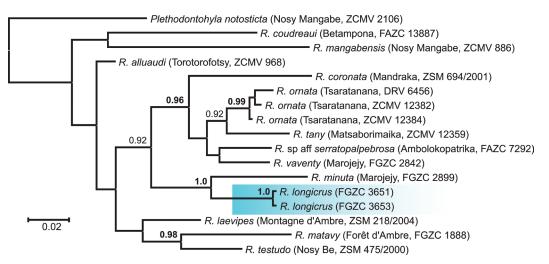


**Figure 2.** Majority-rule consensus tree derived from Bayesian inference analysis of the genus *Rhombophryne* based on the mitochondrial 16S rRNA gene. Numbers at nodes represent posterior probability (PP). PP values greater than 0.95 are bolded. Values lower than 0.8 are not shown.

long branch length indicates, however, a strong genetic differentiation from its probable sister species. Uncorrected pairwise differences (*p*-distances) using the entire amplified 16S fragment (including hypervariable regions; alignment length 536 bp) was 6.8% to *R. minuta* and >8.6% to all other species of *Rhombophryne* (including *R. guentherpetersi*; M. Vences, analyses in progress). The concordance of such a high genetic divergence (>3% in the 16S fragment; see Vieites et al. 2009) with clear morphological differentiation is strong evidence for status as an independent evolutionary lineage, warranting its recognition as a distinct species. We therefore formally describe this new species here as:

### *Rhombophryne longicrus* sp. n.

http://zoobank.org/35E10C49-8211-4E30-BDB0-48E753348738
Figs 3, 4

**Holotype.** ZSM 1630/2012 (FGZC 3653), an adult female with immature oocytes, collected in the montane forest of the Sorata Massif, north Madagascar (ca. 13.675°S, ca. 49.4392°E, ca. 1580 m; datum = WGS84) on 28 November 2012 by A. Rakotoarison, A. Razafimanantsoa, T. Rajoafiarison, F. M. Ratsoavina, O. Hawlitschek and F. Glaw.

**Paratype.** UADBA-A 60271 (FGZC 3651), an adult male with the same collection data as the holotype.

**Diagnosis.** A microhylid assigned to the genus *Rhombophryne* on the basis of overall morphology, including the possession of maxillary and vomerine teeth, absence of expanded toe pads, and absence of an enlarged prepollex. Confirmed as a member of the genus *Rhombophryne* on the basis of its phylogenetic relationships as assessed by mitochondrial DNA, as there are no known morphological characters by which *Rhombophryne* may be distinguished from *Plethodontohyla*.

*Rhombophryne longicrus* sp. n. is distinguished from all other Madagascan frog species by the following set of characters: SVL 23.8–27.9 mm, head wider than long, horizontal tympanum diameter 47% of eye diameter, absence of superciliary spines, weak supratympanic fold, dark supratympanic region and nostril, tibiotarsal articulation reaching the nostril, total hindlimb length 183–185% of SVL, second finger shorter than fourth, and fifth toe shorter than third. It is also separated by a pairwise genetic distance of at least 6.8% in the 16S mitochondrial gene from all other known species of the genus *Rhombophryne*.

Within the genus, *R. longicrus* sp. n. may be distinguished from all *Rhombophryne* species, except *R. laevipes*, *R. minuta*, and *R. vaventy,* by tibiotarsal articulation reaching the nostril (versus not exceeding the eye); from *R. coronata*, *R. ornata*, *R. serratopalpebrosa*, *R. tany*, and *R. vaventy* by the absence of superciliary spines (versus presence); from *R. alluaudi, R. laevipes, R. mat-*

*avy*, *R. testudo*, and *R. vaventy* by its smaller size (SVL 23.8–27.9 mm versus 32–53 mm); from *R. minuta* by its larger size (SVL 23.8–27.9 mm vs. up to 17.1 mm); from *R. testudo* by the absence of barbels on the throat and tympanum smaller than eye; from *R. alluaudi, R. coronata, R. serratopalpebrosa, R. tany*, and *R. vaventy* by its weak, almost absent supratympanic fold; from *R. coudreaui* and *R. vaventy* by smooth dorsal skin (versus granular/tubercular); from *R. mangabensis* by lack of paired dark dorsal tubercles; from *R. laevipes, R. mangabensis, R. ornata, R. testudo*, and *R. vaventy* by absence of dark crossbands on hindlimbs; and from *R. coronata, R. minuta, R. testudo*, and *R. vaventy* by dark supratympanic region.

Osteologically, a micro-CT scanned specimen of *R. longicrus* sp. n. tentatively differs from *R. ornata* (3 specimens: ZSM 1815/2010, 1816/2010, and 2859/2010), *R. serratopalpebrosa* (1 specimen: MNHN 1975.24), *R. tany* (1 specimen: ZSM 1814/2010), and *R. vaventy* (1 specimen: ZSM 375/2005) (as described in Scherz et al. 2014, 2015) by its relatively larger nasals (nasal length at longest point 18.5% of skull length versus 11.1–16.4%), which are in contact with the sphenethmoid (versus not contacting any other bones), its relatively longer and less broad skull (skull length 81.6% of skull width versus 66.5–79.4%), and its relatively longer brain case (frontoparietals+sphenethmoid length 74.0% of skull length versus 63.3–71.5%; length of frontoparietals+sphenethmoid 197.7% of width of frontoparietals anterior to prootic versus 173.4–185.6%). A thorough osteological treatment of this genus is needed to confirm further differences and their values.

*Rhombophryne* species can be confused with *Plethodontohyla* species. *Rhombophryne longicrus* sp. n. differs from them in the following ways: absence of a sharp dorsolateral colour border and expanded finger and toe pads (versus presence in *P. notosticta, P. guentheri, P. mihanika*, and *P. inguinalis*), absence of inguinal spots (versus presence in *P. mihanika, P. inguinalis, P. ocellata*, and *P. bipunctata*), tibiotarsal articulation reaching the nostril (maximally reaching to the mid-eye in all *Plethodontohyla* except *P. mihanika*), absence of crossbands on legs (versus presence in *P. fonetana, P. inguinalis, P. notosticta, P. guentheri*, and *P. mihanika*), and smooth skin (versus granular to rough in *P. tuberata*).

**Description of the holotype.** Adult female in an excellent state of preservation. A ventral incision was made in order to check the sex and access the stomach contents. The incision runs laterally and posteroventrally anterior to the pubis and up the middle of the venter.

Body gracile; dorsal and ventral skin smooth. Head wider than long (HW 122.5% of HL), snout rounded in dorsal view, squarish in lateral view; nostrils weakly protuberant, directed laterally, equidistant between eye and snout; canthus rostralis concave; loreal region concave; tympanum indistinct, oval, horizontally 47% of eye diameter; pupil round; supratympanic fold weak, almost
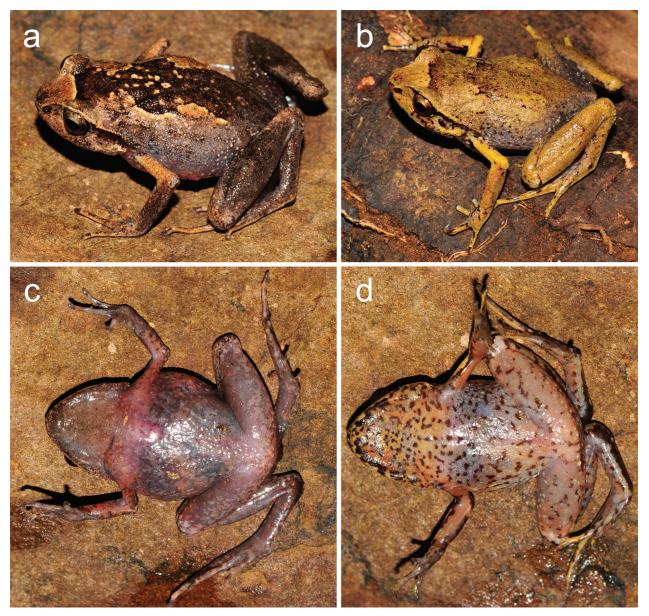
**Figure 3.** *Rhombophryne longicrus* sp. n. in life. Holotype ZSM 1630/2012 in (**a**) dorsolateral and (**c**) ventral view. Paratype UADBA-A 60271 in (**b**) dorsolateral and (**d**) ventral view.

absent; tongue unlobed, posteriorly free; vomerine teeth present in a straight row with a small medial gap (<1 mm; see Osteology below); choanae small, oval.

Arms slender and long; fingers without webbing, long, without distinct subarticular tubercles, relative lengths 1<2<4<3, second finger much shorter than fourth, without enlarged terminal discs; inner metacarpal tubercle present; nuptial pads absent. Legs exceptionally long and slender (HIL 185% of SVL), tibiotarsal articulation reaching the nostril when hindlimb is adpressed along body; toes long, unwebbed, with indistinct subarticular tubercles, relative toe lengths 1<2<5<3<4, third toe much longer than fifth; inner metatarsal tubercle present and indistinct.

Colouration of the holotype: (Fig. 3a, c). In life, snout anterior to eyes, above eyes, side of head, and upper arms bronze to tan in colour; tip of snout darker, lightening posteriorly; area around nostril black; supratympanic region dark brown, fading below to the tan of the lateral side of the head. Body laterally light brown, becoming increasingly yellowish brown dorsolaterally until tan border with dark dorsal marking; this marking is flecked with additional tan spots, and extends from a black horizontal bar between the eyes to the legs, where dark ashy grey dominates; border between dorsal and dorsolateral colouration almost symmetrically emarginated. Hands and feet tan with dark flecks. Ventral skin pinkish and slightly translucent; chin dark relative to rest of venter, posteriorly lightening with few darker patches interspersed with translucent areas lacking pigment. Anteroventral surface of legs with dark pigment, becoming less pigmented more ventrally; ventral surface mottled pinkish and light brown.

After three years in 70% ethanol, all browns have faded to shades of grey. Dorsal areas that were lightest in shade
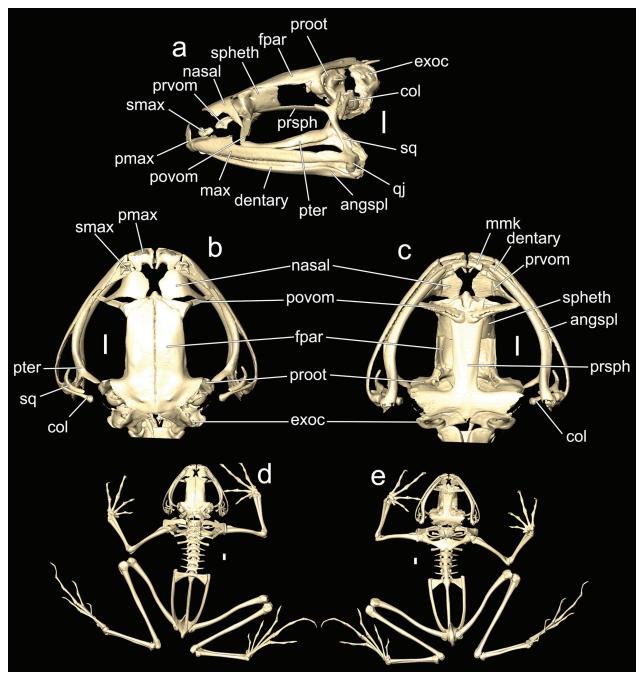
**Figure 4.** Osteology of the holotype of *Rhombophryne longicrus*, ZSM 1630/2012. Skull in (**a**) lateral, (**b**) dorsal, and (**c**) ventral view. Skeleton in (**d**) dorsal and (**e**) ventral view. Note: figures display only calcified structures; cartilages are omitted due to limitations of micro-CT scanning. Abbreviations: angspl = angulosplenial, col = columella, exoc = exoccipital, fpar = frontoparietal, max = maxillary, mmk = mentomeckelian, pmax = premaxilla, povom = postchoanal vomer+neopalatine, proot = prootic, prsph = parasphenoid, prvom = prechoanal vomer, pter = pterygoid, qj = quadratojugal, smax = septomaxilla, spheth = sphenethmoid, sq = squamosal.

are whitish, particularly between the eyes anterior to the dark inter-ocular bar. Ventrally, all areas that lack pigmentation and were pink in life are cream in preservation. Chin the same colour as the snout.

Osteology of the holotype: (Fig. 4, Suppl. material 1). All bones of the skull paired except the parasphenoid and sphenethmoid. Vomer divided into pre- and postchoanal portions; prechoanal part small, longer than broad, subtri-

angular; postchoanal part overlapping neopalatine, bearing ventral serrations (vomerine teeth), separated medially from its counterpart by a gap of 0.7 mm. Postchoanal vomer+neopalatine in dorsal contact with anterior end of cultriform process of parasphenoid, and through it with the sphenethmoid; laterally not in contact with maxilla. Teeth present on maxilla and premaxilla. Premaxilla medially not fused to counterpart, anterodorsal alary processes

rising dorsolaterally, pars palatina with two well-defined processes, the medial (palatine) process thin, lateral process broad; pars dentalis bearing small teeth. Septomaxilla roughly spiralling upward from posterior ramus to lateral ramus to anterior ramus to medial ramus. Nasal medially in contact with the sphenethmoid posteriorly, possessing a pointed maxillary process extending ventrolaterally toward the maxilla, lacking an anterolateral ramus. Maxilla long, bearing small, poorly resolved teeth, possessing a horizontal pars palatina along its lingual margin; in broad lateral contact with anterior ramus of pterygoid; posteriorly without clear distinction from quadratojugal. Pterygoid broad and triradiate, with anterior, medial, and posterior rami; the ventrolateral edge of its anterior ramus, posterior margin of its medial ramus, and lateral face of its posterior ramus sculpted inward; medial ramus much shorter than posterior ramus; posterior ramus not in contact with quadratojugal. Quadratojugal L-shaped, anterior process without clear distinction from posterior of maxilla; posteriorly possessing a ventral bulbous process with a concave posterior face; dorsally without clear distinction from squamosal. Squamosal thin and distally bifurcated, extending anterodorsomedially from quadratojugal to level of otic capsule passing anterior to columella; otic ramus longer than zygomatic ramus. Columella with a long shaft that exceeds the level of the squamosal; dorsal edge of columella straight even to end of footplate; columellar footplate broad and concave. Frontoparietal medial and lateral edges straight and parallel, lateral edge curved ventrally to form dorsolateral border of brain case; possessing paired bumps at the transverse level of the columellae; posterolateral sutures with prootics and exoccipitals not clear from micro-CT scans; anterior process contacting sphenethmoid. Parasphenoid T-shaped; cultriform process broadening anteriorly, contacting sphenethmoid at its anterior end; broad posterior alary processes perpendicular to cultriform process, in dorsal contact with prootics anteriorly and exoccipitals posteriorly.

Mandible slim, edentate. Mentomeckelian small, in narrow medial contact with counterpart (possibly artefactual), and in dorsolateral contact with dentary. Dentary long and thin with a sculpted outer face and smooth inner face, overlapping angulosplenial for much of its length. Angulosplenial broadening posteriorly, with a posterior dorsomedial crista; possessing a lateral channel running from the posterior into the sculpted outer edge of the dentary.

Posterolateral processes of hyoid shovel-like, a medial crista running along posteromedial process, the base of which is broad and flat with a rounded anteromedial edge and sharp anterolateral and posteromedial corners; parahyoid absent.

Humerus long, slim and straight; crista lateralis weak, crista ventralis short (~30% of humerus length), crista medialis absent. Radioulna broadening distally. Finger phalangeal formula 2-2-3-3. Terminal phalanges of fingers 2, 3, and 4 with distal knobs. Prepollex 31% of first finger.

Pectoral girdle composed of paired coracoids, clavicles, scapulae, cleithra and suprascapulae. Sternal characters not visible in CT render. Coracoids in medial contact; medially dorsoventrally flattened, laterally rounded, posterior surface straight, anterior surface strongly concave. Clavicle thin and curved approximately parallel to the anterior edge of the coracoid, its lateral end broadened, posteriorly in contact with ventral edge of scapular pars acromialis. Scapula thick, hourglass shaped, its posterior edge less strongly curved than its anterior edge, medioventrally bifurcated; pars acromialis distally rounded, in contact with the lateral end of the clavicle, its anterior surface concave; pars glenoidalis curved ventrally, in contact with lateral face of coracoid, posterior face concave; dorsal edge of scapula approaching cleithrum. Cleithrum thin and long, not possessing any cristae, anteriorly thicker than posteriorly. Suprascapula with highest X-ray absorption ventrally and posteriorly suggesting possible ossification in these areas.

Toe phalangeal formula 2-2-3-4-3; terminal phalanges without distinct distal knobs. Leg bones long and thin. Femur without any crests. Tibiofibula slightly longer than femur. Tibiale and fibulare proximally and distally fused, articulating distally with metatarsals V and IV, tarsals 1–3, and the centrale. Prehallux present, short.

Ilium, ischium, and pubis forming ossified acetabulum, each composed of paired, medially fused elements. Iliac shafts oval in cross-section, dorsal-ventral diameter larger, possessing a weak dorsal tubercle posterior to shallow oblique groove. Iliosacral articulation type IIA sensu Emerson (1979).

Eight presacrals present; no vertebrae fused. Posterior articular processes round. Transverse processes of presacrals II–IV broader than those of V–VIII. Neural spines decreasing in size from presacral II to absent by V. Sacrum wide, with broad diapophyses articulating with the ilia; anterior edge of each diapophysis roughly perpendicular to body axis, posterior edge oblique. Urostyle long and thin, with a dorsal ridge along a third of its length, beginning at its anterior end; articulation with sacrum bicondylar.

**Measurements.** Holotype (paratype in brackets), measurements in mm: SVL 28.0 (23.8), HW 9.9 (9.7), HL 8.0 (7.0), ED 3.3 (2.8), END 2.0 (2.0), NSD 1.9 (1.7), NND 3.0 (2.2), TDH 1.5 (1.3), TDV 1.8 (1.4), HAL 8.4 (7.0), UAL 5.7 (4.7), LAL 6.8 (5.7), FORL 20.9 (17.4), THIL 13.2 (11.7), THIW 3.9 (3.4), TIBL 14.6 (11.7), TIBW 2.97 (2.64) TARL 8.6 (7.3), FOL 14.8 (12.5), FOTL 23.4 (19.8), HIL 51.2 (43.2), IMCL 1.0 (0.9), IMTL 1.3 (1.0).

**Variation.** Only two specimens are known. The paratype is male, and smaller than the holotype (SVL 23.8 mm). It agrees in all aspects of its morphology with the holotype, but differs strongly in colouration (see Fig. 3b, d). In life, the dorsum has a yellow-brown base colour, with distributed black or dark brown flecks. A black inter-ocular bar is present, behind which the skin fades from brown to the base colour; the back does not possess the dark marking of the holotype, but instead two darker areas with a few black

flecks lie in the suprascapular region. The lateral skin fades to grey ventrally, also speckled with black. A dark line runs from the preocular region to the axial pit through the supraocular and supratympanic regions. The nostril is surrounded by black, and the tympanum has a dark fleck on it. The legs are grey at the hip, but this lightens to the yellowish brown of the dorsum further away; the arms are dorsally yellow, the hands possessing a few black spots. Ventrally, the pink areas of the holotype are orange in life in the paratype, particularly over the pectoral girdle and beneath the chin. The venter is marked with many irregular black flecks. The arms are ventrally orange, bordered posteriorly in black.

**Etymology.** The species epithet is an invariable noun in apposition to the genus name, derived from the Latin words *longus* (meaning long), and *crus* (meaning leg), and refers to the unusually long legs of this species.

**Distribution.** This species has only been found at high altitude in the montane forests of the Sorata massif in north Madagascar. Its distinctiveness leads us to hypothesize that it has never been found elsewhere and misidentified, so it may be microendemic to this small area. Additional surveys are required in areas in and around Sorata to identify its full distribution.

**Ecology.** Both specimens described here were captured in the early evening on the ground along a path through primary montane forest. The stomachs of both specimens contained remains of several small insects (mostly Coleoptera) and a spider (possibly belonging to the family Salticidae), mixed with moss, suggesting an opportunistic diet of arthropods. Calls of this species are unknown. The female holotype had more than twenty immature oocytes with the largest having diameters ranging from 1.3 to 1.6 mm. As a member of the Cophylinae, it is likely that *R. longicrus* lays its eggs away from running water or large water bodies, and has endotrophic tadpoles.

**Conservation status.** The forests of Sorata are currently unprotected. All locally endemic species are threatened by uninhibited deforestation and forest degradation. The greatest pressure on forests is at their edges. High altitude species like *R. longicrus* may therefore be the least threatened by this. However, a sustained rate of deforestation will increase the threat level to species at ever-higher altitudes. It is conceivable that a restriction of this species to high altitudes may mean that it is susceptible to climate change (Raxworthy 2008, Raxworthy et al. 2008). We consider this threat far less serious than that of deforestation. *Batrachochytrium dendrobatidis* has now been confirmed from numerous localities in Madagascar (Bletz et al. 2015). So far no negative impacts on native frogs have been observed. The water-independent lifestyle of *Rhombophryne* species suggests that they are probably at relatively low threat from chytridiomycosis.

While this species is, at present, known from just two specimens collected on one expedition, the fact that it has not been collected by previous expeditions suggests it may be scarce, seasonal, or have a scattered distribution. Even if it were distributed throughout the forests of the Sorata massif, its distribution would still only constitute an area of ~250 km² (as calculated in Google Earth® Pro 6.1.0.500, Google Inc., Mountain View, CA). Thus, because of its potentially limited range inside an unprotected forest, the on-going and intensifying threat of deforestation, potential threat by climate change, and potential scarcity or seasonality, it qualifies as Endangered B1ab(iii) under the IUCN Red List Criteria (2012).

## Discussion

Hindlimb length is significantly associated with habitat and mode of life in frogs (Gomes et al. 2009). Longer legs relative to body length result in greater relative leaping performance (Zug 1978, Choi et al. 2003, Gomes et al. 2009). In general, fossorial frogs have the poorest jumping performance, while arboreal and semi-aquatic frogs are the strongest jumpers (Zug 1978). Terrestrial frogs are intermediate, but generally poor leapers, preferring to hop rather than leap. Emerson (1976) noted that adaptations involved in hopping in terrestrial frogs are similar to those required for burrowing. This can lead to difficulties disentangling the morphology involved in these two habits. We may also expect this to lead to frequent evolutionary transitions in preference between hopping and digging.

Robust and at least partly burrowing frogs typify the genus *Rhombophryne*. Some species are specialised burrowers (*R. matavy* and *R. testudo*), while others are probably facultative burrowers (*R. serratopalpebrosa* group, and probably *R. alluaudi*, *R. laevipes*, and *R. mangabensis*). Two species however seem to have at least partly abandoned burrowing: *R. minuta* and *R. longicrus*. *Rhombophryne minuta* lives at high altitude (close to and above the tree line) on the Marojejy massif and calls from low bushes that make up the complex matrix of ground in its unusual habitat (Glaw and Vences 2007). *Rhombophryne longicrus* lives at high altitude on the Sorata Massif to the north of Marojejy; its ecology is more or less unknown. These species form a strongly supported sister group in our phylogeny (Fig. 2), and resemble each other in morphology. Most notably, both have exceptionally long, slender legs relative to those of their congeners: HILs of both species are between 178.5% and 183.8% of their SVLs, considerably above the genus mean of 158.0%; and relative to their lengths, the thighs of *R. longicrus* are thinner than any other *Rhombophryne* species (THIW 29.1–29.2% of THIL) except *R. minuta* (whose THIW/THIL ranges from 24.4–38.0%; Scherz et al. unpublished data). We therefore expect these frogs to be capable of leaps of relatively greater distance than their congeners.

In addition to leg length, several other characters are also associated with more saltatorial locomotion. Emer-

son (1979) characterised three types of iliosacral articulation correlated with locomotion patterns: Type I, expanded sacral diapophyses without ligament attachment, allowing great anteroposterior freedom of movement, most common in aquatic frogs, but also found in burrowers and climbers (Reilly and Jorgensen 2011); Type IIA, broad sacral diapophyses and proximal attachment of a broad ligament, the most adaptable and widespread of the articulation types, typical of walking and hopping locomotion, common in burrowers; and Type IIB, distal attachment of a narrow ligament to thin and posteriorly pointed sacral diapophyses, typical of long-distance leapers (although frogs with this type of articulation are not necessarily better leapers; see Reilly and Jorgensen 2011). Reilly and Jorgensen (2011) expanded this classification into seven types, by incorporating also dorsal ridges of the iliac shafts, and the nature of the urostyle. The iliosacral articulation of *R. longicrus* is Type IIA sensu Emerson (1979), and the ilia possess no ridges, while the urostyle is bicondylar and bears a ridge on its anterior third (as in all other *Rhombophryne* spp. so far investigated).

The iliosacral articulation of *Rhombophryne longicrus* is almost the same as members of the *R. serratopalpebrosa* group (Scherz et al. 2014, 2015), but is slightly modified such that its iliac shafts are closer together. This may produce faster launch speeds and thus greater leaping distances (Choi et al. 2003). This, coupled with its long, slim legs and lack of burrowing specialisations, such as enlarged internal metatarsal tubercles, suggests adaptation to saltatorial locomotion. In external morphology, and based on preliminary osteological data, its sister species, *R. minuta*, appears to share most of these characteristics. Therefore, we hypothesise that these two species constitute a divergent, ancestrally saltatorial lineage that diverged from possibly semi-fossorial ancestors. A thorough treatment of the osteology of *Rhombophryne* will shed light on this question. It is clear already, however, that this genus constitutes an osteologically and ecologically diverse group of frogs, rivalling the diversity seen in other cophylines.

The discovery of such a distinctive new species highlights the incompleteness and patchiness of herpetological survey work in Madagascar. Whilst some forests, particularly accessible, protected ones, are receiving a lot of research attention (e.g. Betampona: Andreone et al. 2010; Rosa et al. 2012, 2014), others, like the forests of the Sorata massif, are receiving little study. Sorata is part of a constellation of high-altitude massifs, linked to the massifs Tsaratanana to the west, and Marojejy to the east by narrow stretches of remaining forest. Further survey work will be needed to understand its diversity and role in this network of massifs. At the same time, however, its forests are unprotected and highly threatened by anthropogenic habitat destruction and modification. Protected status must therefore be pursued together with an enhanced knowledge of this area's flora and fauna.

## References

Andreone F, Rosa GM, Noel J, Crottini A, Vences M, Raxworthy CJ (2010) Living within fallen palm leaves: the discovery of an unknown *Blommersia* (Mantellidae: Anura) reveals a new reproductive strategy in the amphibians of Madagascar. Naturwissenschaften 97(6): 525–543. doi: 10.1007/s00114-010-0667-x

Andreone F, Vences M, Vieites DR, Glaw F, Meyer A (2005) Recurrent ecological adaptations revealed through a molecular analysis of the secretive cophyline frogs of Madagascar. Molecular Phylogenetics and Evolution 34(2): 315–322. doi: 10.1016/j.ympev.2004.10.013

Bletz MC, Rosa GM, Andreone F, Courtois EA, Schmeller DS, Rabibisoa NHC, Rabemananjara FCE, Raharivololoniaina L, Vences M, Weldon C, Edmonds D, Raxworthy CJ, Harris RN, Fisher MC, Crottini A (2015) Widespread presence of the pathogenic fungus *Batrachochytrium dendrobatidis* in wild amphibian communities in Madagascar. Scientific Reports 5(8633): 1–10. doi: 10.1038/srep08633

Bruford MW, Hanotte O, Brookefield JFY, Burke T (1992) Single-locus and multilocus DNA fingerprint. In: Hoelzel AR (Ed.) Molecular Genetic Analysis of Populations: A Practical Approach. IRL Press, Oxford, 225–270.

Choi I, Shim JH, Ricklefs RE (2003) Morphometric relationships of take-off speed in anuran amphibians. Journal of Experimental Zoology 299A: 99–102. doi: 10.1002/jez.a.10293

D'Cruze N, Köhler J, Vences M, Glaw F (2010) A new fat fossorial frog (Microhylidae: Cophylinae: *Rhombophryne*) from the rainforest of the Forêt d'Ambre Special Reserve, northern Madagascar. Herpetologica 66(2): 182–191. doi: 10.1655/09-008r1.1

Darriba D, Taboada GL, Doallo R, Posada D (2012) jModelTest 2: more models, new heuristics and parallel computing. Nature Methods 9: 772. doi: 10.1038/nmeth.2109

Emerson SB (1976) Burrowing in frogs. Journal of Morphology 149(4): 437–458. doi: 10.1002/jmor.1051490402

Emerson SB (1979) The ilio-sacral articulation in frogs: form and function. Biological Journal of the Linnean Society 11: 153–168. doi: 10.1111/j.1095-8312.1979.tb00032.x

Glaw F, Köhler J, Vences M (2010) A new fossorial frog, genus *Rhombophryne*, from Nosy Mangabe Special Reserve, Madagascar. Zoosystematics and Evolution 86(2): 235–243. doi: 10.1002/zoos.201000006

Glaw F, Vences M (2007) A Field Guide to the Amphibians and Reptiles of Madagascar. 3rd edition. Vences & Glaw Verlags GbR, Köln, Germany.

Gomes FR, Rezende EL, Grizante MB, Navas CA (2009) The evolution of jumping performance in anurans: morphological correlates and ecological implications. Journal of Evolutionary Biology 22: 1088–1097. doi: 10.1111/j.1420-9101.2009.01718.x

ICZN (1999) International Code of Zoological Nomenclature. 4th Edition. The International Trust for Zoological Nomenclature, London, 306 pp.

IUCN (2012) IUCN Red List Categories and Criteria: Version 3.1. IUCN, Gland, Switzerland and Cambridge, UK.

Noble GK, Parker HW (1926) A synopsis of the brevicipitid toads of Madagascar. American Museum Novitates 232: 1–21.

Palumbi SR, Martin A, Romano S, McMillan WO, Stice L, Grabowski G (1991) The Simple Fool's Guide to PCR, Version 2.0. Privately published, University of Hawaii.

Parker HW (1934) Monograph of the frogs of the family Microhylidae. Trustees of the British Museum, London, UK.

Peloso PLV, Frost DR, Richards SJ, Rodrigues MT, Donnellan S, Matsui M, Raxworthy CJ, Biju SD, Lemmon EM, Lemmon AR, Wheeler WC (2015) The impact of anchored phylogenomics and taxon sampling on phylogenetic inference in narrow-mouthed frogs (Anura, Microhylidae). Cladistics. doi: 10.1111/cla.12118

Perl RGB, Nagy ZT, Sonet G, Glaw F, Wollenberg KC, Vences M (2014) DNA barcoding Madagascar's amphibian fauna. Amphibia-Reptilia 35: 197–206. doi: 10.1163/15685381-00002942

Rambaut A, Suchard MA, Xie D, Drummond AJ (2014) Tracer v1.6. http://beast.bio.ed.ac.uk/Tracer

Raxworthy CJ (2008) Global warming and extinction risks for amphibians in Madagascar: a preliminary assessment of upslope displacement. In: Andreone F (Ed.) A Conservation Strategy for the Amphibians of Madagascar. Monografie. Museo Regionale di Scienze Naturali, Torino, 67–84.

Raxworthy CJ, Pearson RG, Rabibisoa N, Rakotondrazafy AM, Ramanamanjato J-B, Raselimanana AP, Wu S, Nussbaum RA, Stone DA (2008) Extinction vulnerability of tropical montane endemism from warming and upslope displacement: a preliminary appraisal for the highest massif in Madagascar. Global Change Biology 14(8): 1703–1720. doi: 10.1111/j.1365-2486.2008.01596.x

Reilly SM, Jorgensen ME (2011) The evolution of jumping in frogs: Morphological evidence for the basal anuran locomotor condition and the radiation of locomotor systems in crown group anurans. Journal of Morphology 272: 149–168. doi: 10.1002/jmor.10902

Ronquist F, Teslenko M, van der Mark P, Ayres DL, Darling A, Höhna S, Larget B, Liu L, Suchard MA, Huelsenbeck JP (2012) MR-BAYES 3.2: Efficient Bayesian phylogenetic inference and model selection across a large model space. Systematic Biology 61(3): 539–542. doi: 10.1093/sysbio/sys029

Rosa GM, Andreone F, Crottini A, Hauswaldt JS, Noël J, Rabibisoa NH, Randriambahiniarime MO, Rebelo R, Raxworthy CJ (2012) The amphibians of the relict Betampona low-elevation rainforest, eastern Madagascar: an application of the integrative taxonomy approach to biodiversity assessments. Biodiversity and Conservation 21(6): 1531–1559. doi: 10.1007/s10531-012-0262-x

Rosa GM, Crottini A, Noël J, Rabibisoa N, Raxworthy CJ, Andreone F (2014) A new phytotelmic species of *Platypelis* (Microhylidae: Cophylinae) from the Betampona Reserve, eastern Madagascar. Salamandra 50(4): 201–214.

Scherz MD, Ruthensteiner B, Vences M, Glaw F (2014) A new microhylid frog, genus *Rhombophryne*, from northeastern Madagascar, and a re-description of *R. serratopalpebrosa* using micro-computed tomography. Zootaxa 3860(6): 547–560. doi: 10.11646/zootaxa.3860.6.3

Scherz MD, Ruthensteiner B, Vieites DR, Vences M, Glaw F (2015) Two new microhylid frogs of the genus *Rhombophryne* with superciliary spines from the Tsaratanana Massif in northern Madagascar. Herpetologica, in press.

Schneider CA, Rasband WS, Eliceiri KW (2012) NIH Image to ImageJ: 25 years of image analysis. Nature Methods 9: 671–675. doi: 10.1038/nmeth.2089

Trueb L (1968) Cranial osteology of the hylid frog, *Smilisca baudini*. University of Kansas Publications Museum of Natural History 18:11–35.

Trueb L (1993) Patterns of cranial diversity among the Lissamphibia. In: Hanken J, Hall BK (Eds) The Skull, Vol. 2. Patterns of Structural and Systematic Diversity University of Chicago Press, USA, 255–343

Vieites DR, Wollenberg KC, Andreone F, Köhler J, Glaw F, Vences M (2009) Vast underestimation of Madagascar's biodiversity evidenced by an integrative amphibian inventory. PNAS 106(20): 8267–8272. doi: 10.1073/pnas.0810821106

Wollenberg KC, Vieites DR, van der Meijden A, Glaw F, Cannatella DC, Vences M (2008) Patterns of endemism and species richness in Malagasy cophyline frogs support a key role of mountainous areas for speciation. Evolution 62(8): 1890–1907. doi: 10.1111/j.1558-5646.2008.00420.x

Zug GR (1978) Anuran locomotion – structure and function, 2: jumping performance of semiaquatic, terrestrial, and arboreal frogs. Smithsonian Contributions to Zoology 276: 1–31. doi: 10.5479/si.00810282.276

# Supplementary material 1

### PDF-embedded 3D Skeletal Model

Authors: Mark D. Scherz, Andolalao Rakotoarison, Oliver Hawlitschek, Miguel Vences, Frank Glaw

Data type: Adobe PDF file

Explanation note: This file contains a PDF-embedded interactive 3D model of the skeleton of the holotype of *Rhombophryne longicrus* sp. n., ZSM 1630/2012, generated via X-ray micro-Computed Tomography. The model can be opened in Adobe® Acrobat Pro or Reader, versions IX and above